Biochimica et Biophysica Acta 1838 (2014) 328–338

Contents lists available at ScienceDirect

Biochimica et Biophysica Acta

journal homepage: www.elsevier.com/locate/bbamem

Ion channel stability of Gramicidin A in lipid bilayers: Effect of hydrophobic mismatch

Ipsita Basu [a], Amitabha Chattopadhyay [b,*], Chaitali Mukhopadhyay [a,*]

[a] Department of Chemistry, University of Calcutta, 92, A. P. C. Road, Kolkata 700009, India
[b] Centre for Cellular & Molecular Biology, Uppal Road, Hyderabad 500007, India

ARTICLE INFO

Article history:
Received 27 June 2013
Received in revised form 20 September 2013
Accepted 3 October 2013
Available online 11 October 2013

Keywords:
Gramicidin A
DAPC bilayer
Negative hydrophobic mismatch
Ion channel stability

ABSTRACT

Hydrophobic mismatch which is defined as the difference between the lipid hydrophobic thickness and the peptide hydrophobic length is known to be responsible in altering the lipid/protein dynamics. Gramicidin A (gA), a 15 residue β helical peptide which is well recognized to form ion conducting channels in lipid bilayer, may change its structure and function in a hydrophobic mismatched condition. We have performed molecular dynamics simulations of gA dimer in phospholipid bilayers to investigate whether or not the conversion from channel to non-channel form of gA dimer would occur under extreme negative hydrophobic mismatch. By varying the length of lipid bilayers from DLPC (1, 2-Dilauroyl-sn-glycero-3-phosphocholine) to DAPC (1, 2-Diarachidoyl-sn-glycero-3-phosphocholine), a broad range of mismatch was considered from nearly matching to extremely negative. Our simulations revealed that though the ion-channel conformation is retained by gA under a lesser mismatched situation, in extremely negative mismatched situation, in addition to bilayer thinning, the conformation of gA is changed and converted to a non-channel one. Our results demonstrate that although the channel conformation of Gramicidin A is the most stable structure, it is possible for gA to change its conformation from channel to non-channel depending upon the local environment of host bilayers.

1. Introduction

Membrane protein interaction study has been the focal area in cell research for a long time. The way proteins interact with the membrane in which it is embedded may affect the structural and functional properties of both the proteins and the membrane lipids [1]. One key factor that influences such interaction is hydrophobic mismatch [2] which is defined as the difference between the hydrophobic length of the transmembrane segment of the protein and the hydrophobic width of the lipid bilayer [3]. Depending upon the extent, hydrophobic mismatch can cause a number of responses in the membrane/protein system, involving local bilayer thinning in case of negative mismatch (i.e. peptide hydrophobic length is smaller than that of the lipid bilayer), local bilayer stretching in case of positive mismatch (when peptide hydrophobic length is larger than that of the lipid bilayer) [3], lipid sorting in mixed lipid bilayers [4], peptide unwinding, peptide tilting, peptide aggregation [5], etc. Hydrophobic mismatch becomes more relevant specifically for ion channels like gramicidin where the channel activity is directly related to the conformation of the protein in the bilayer.

The linear gramicidins, a family of linear pentadecapeptide antibiotics, form cation selective channels in model membranes [6]. Gramicidin can increase the permeability of various membranes to monovalent cations which seems to be responsible for their antibacterial activity [7,8]. Due to its relatively small size and easy availability, it serves as an excellent model for transmembrane channels [9]. The unique sequence of gramicidin of alternating D and L amino acids makes it sharply different from other proteins, most of which are exclusively composed of L amino acids [9–11]. The natural mixture of gramicidin comprises predominantly Gramicidin A (85%) [7] which is one of the most hydrophobic sequences known [12]. The unique sequence of gramicidin helps it to adopt a wide range of conformations depending upon the local environment among which two main motifs are identified: 1) the single stranded head to head $\beta^{6.3}$ helix (channel form) [13] and 2) the double stranded intertwined helix (collectively known as the non-channel form) [14]. Although the channel form is the thermodynamically preferred conformation [15,16], the non-channel forms have also been shown to exist in membranes with polyunsaturated acyl tail or with large acyl chain length [16–19]. The channel activity of gramicidin has been shown to reduce in membranes with increased thickness [20]. Experimental evidence also suggests that under extreme hydrophobic mismatch the channel conformer of Gramicidin A ultimately converts to non-channel forms [19].

A recent work by Allen and de Jesus. listed the determinants of hydrophobic mismatch responses for transmembrane helices containing

* Corresponding authors.
E-mail addresses: amit@ccmb.res.in (A. Chattopadhyay), chaitalicu@yahoo.com, cmchem@caluniv.ac.in (C. Mukhopadhyay).

0005-2736/$ – see front matter © 2013 Elsevier B.V. All rights reserved.
http://dx.doi.org/10.1016/j.bbamem.2013.10.005

tryptophan residues [21]. They have reported that tilting is the dominant response in positive mismatch and in negative mismatch it is local bilayer thinning. They have also shown that with the increase in the number of anchoring tryptophan residues, thinning increases in negative mismatch as there are more residues to prefer the membrane interfacial region. Another recent work on hydrophobic mismatch suggested that helices adopt mainly via changing their tilt angle in positive mismatch, however, the mechanism varies with the peptide sequence in the flanking region [22]. Recently a three-dimensional stress field around the gA dimer in lipid bilayers that feature different degrees of negative hydrophobic mismatch was computed using both all atom and coarse grain MD simulations [23]. Stress field distribution helps in highlighting the tryptophan residues at the protein/membrane/water interface as mechanical anchors. Influence of hydrophobic mismatch on the structure and dynamics of gA has been reported by Im et al. [24] showing that the channel structure varied little with changes in hydrophobic mismatch. In earlier studies using solid-state NMR spectroscopy of ^{13}C-labelled analogues of gramicidin in oriented multilayers of phosphatidylcholine, Cornell et al. showed that variation of the lipid hydrocarbon chain length has no effect on the structure or orientation of the peptide backbone [25]. However their study did not include very thick lipid bilayer, so the actual mechanism of the channel to non-channel conformational transition in the presence of very thick membranes remains poorly understood. To explore the structure and function of gA under extreme mismatch situations, we present an all atom molecular dynamics simulation of the channel conformer of gA in DAPC bilayer along with DLPC, DMPC and POPC lipid bilayers.

The main focus in this work is to study the alteration in the structure and dynamics of gA and the lipids under different degrees of hydrophobic mismatch. The hydrocarbon chain of lipid is varied from twelve to twenty carbons in length to create different situations from nearly matched to extreme negatively mismatched. The structural conversion of gA in extremely mismatched situation as well as the local structural adaptations in bilayer systems by which they alleviate the imposed hydrophobic mismatch is shown here. We observed that local bilayer thinning is the main response to hydrophobic mismatch but it is not sufficient to compensate the mismatch in the case of very thick membranes. It was shown experimentally by Mobashery et al. that the channel structure of gramicidin is disrupted in DEPC (dierucoylphosphatidylcholine) lipid bilayer [26] which has 22 carbon atoms in its acyl chain i.e. in a very thick lipid the channel activity is lost, while the structure is preserved in thinner bilayers. It was also shown earlier that gramicidin conformation shifts toward non-channel conformations in extremely thick gel phase membranes, e.g. in DAPC, although it is not excluded from the membrane [19]. We have used DAPC lipid as one of our model systems because it has 20 carbon atoms in its acyl tail and even at this length we have observed a channel to non-channel transition. The present results point toward several adaptations like local bilayer hydrophobic thinning, changes in area per lipid, area compressibility modulus, protein secondary structure change etc, as well as the indication of channel distortion.

2. Computational methodology

2.1. System setup

The atomistic simulations were performed using NAMD_2.7 [27] package with the standard CHARMM27 force field [28] including dihedral cross term corrections (CMAP) [29]. We use four different lipids like 1, 2-Dilauroyl-sn-glycero-3-phosphocholine (DLPC), 1, 2-Dimyristoyl-sn-glycero-3-phosphocholine (DMPC), 1-palmitoyl-2-oleoyl-phophatidylcholine (POPC) and 1, 2-Diarachidoyl-sn-glycero-3-phosphocholine (DAPC) as the component of four different bilayers. Each model bilayers is consisted of 128 lipids and these bilayers are built using a CHARMM-GUI membrane builder [30] except for DAPC which is built using the software 'Insight II' (Accelrys Inc., USA) running on a Silicon Graphics O2. TIP3P water model was used [31]. The coordinate of the channel conformer of Gramicidin A was taken from the Protein data bank (PDB entry: 1MAG) [32] and this is placed vertically inside the membrane such as that at least the C-terminal tryptophan residues of one monomer could be placed at the bilayer interface as it is the preferred location of tryptophan residues [33]. We define the two monomers as monomer 1 and monomer 2 where monomer 2 is placed near the interface (Fig. S11 in the Supporting Information). To insert a gA dimer in each lipid bilayer, two overlapping lipids from each monolayer of the membrane were removed such that no lipids penetrate the gA dimer. Then KCl was added to maintain the physiological salt concentration of 150 mM. Prior to free MD simulations, the systems were energy minimized to remove the unwanted overlaps and to relax the system followed by a 130 ns production run for each system in which the protein backbone was fixed for the first 30 ns which is considered as the equilibration period. We also simulated a pure DAPC bilayer for 120 ns as control simulation.

2.2. Simulation protocol

All MD simulations were carried out under the isobaric–isothermal (NPT) ensemble with imposed 3D periodic boundary conditions. A time step of 1 fs is used to integrate the equation of motion. The temperature was maintained at 300 K for all simulations using the Langevin dynamics, while the pressure was kept constant at 1 bar using a Nośe-Hoover-Langevin piston [34]. This temperature is both physiologically relevant and above the phase transition temperature of DLPC, DMPC, and POPC [19,35]. For DAPC the phase transition temperature is above 300 K. Hence DAPC lipid bilayer at 300 K will remain in gel phase [19]. As we do not want any effect of temperature on our simulation results, the temperature is kept fixed at 300 K. So we had done the simulation of DAPC system at gel phase. Moreover we have experimental data of DAPC at gel phase thus we can compare the simulation results with the experimental data. The smooth particle mesh Ewald method was used to calculate long range electrostatic calculations [36]. Short range interactions were cutoff at 10 Å. All bond lengths involving hydrogen atoms were held fixed using the RATTLE [37] and SETTLE algorithms [38]. The trajectory analysis was performed with CHARMM (Chemistry at Harvard Macromolecular Mechanics) [39] and the snapshots were generated by VMD [40]. It should be noted that the initial 30 ns equilibration when the gA backbone was fixed was not included in the data analysis.

3. Results and discussion

To study the effect of varying hydrophobic mismatch, we have used different phosphatidylcholines (PC), having different saturated fatty acid lengths from C12:0 to C20:0 including a monounsaturated PC. Our major focus is on the responses of the peptide as well as on the membrane under negative mismatch circumstances. The results of lipid and peptide adaptations are divided into two sections.

3.1. Membrane responses

The most prominent response by which the system can alleviate the imposed hydrophobic mismatch is the alteration of membrane thickness which occurs due to local lipid adjustment. We have defined the average hydrophobic thickness as the distance between the acyl chain C2 carbon atoms of the two opposing bilayer leaflets [41]. The snapshots in Fig. 1 show the changes in the systems before and after the simulations. To estimate the alterations, lipids were classified into two categories based on distance criterion: if any heavy atom of a lipid lies within 5 Å from any backbone atom of the peptide it is defined as local lipid and the rest is bulk lipid [3]. The hydrophobic thickness of two different categories of lipids was calculated separately and it is discussed in the next section.

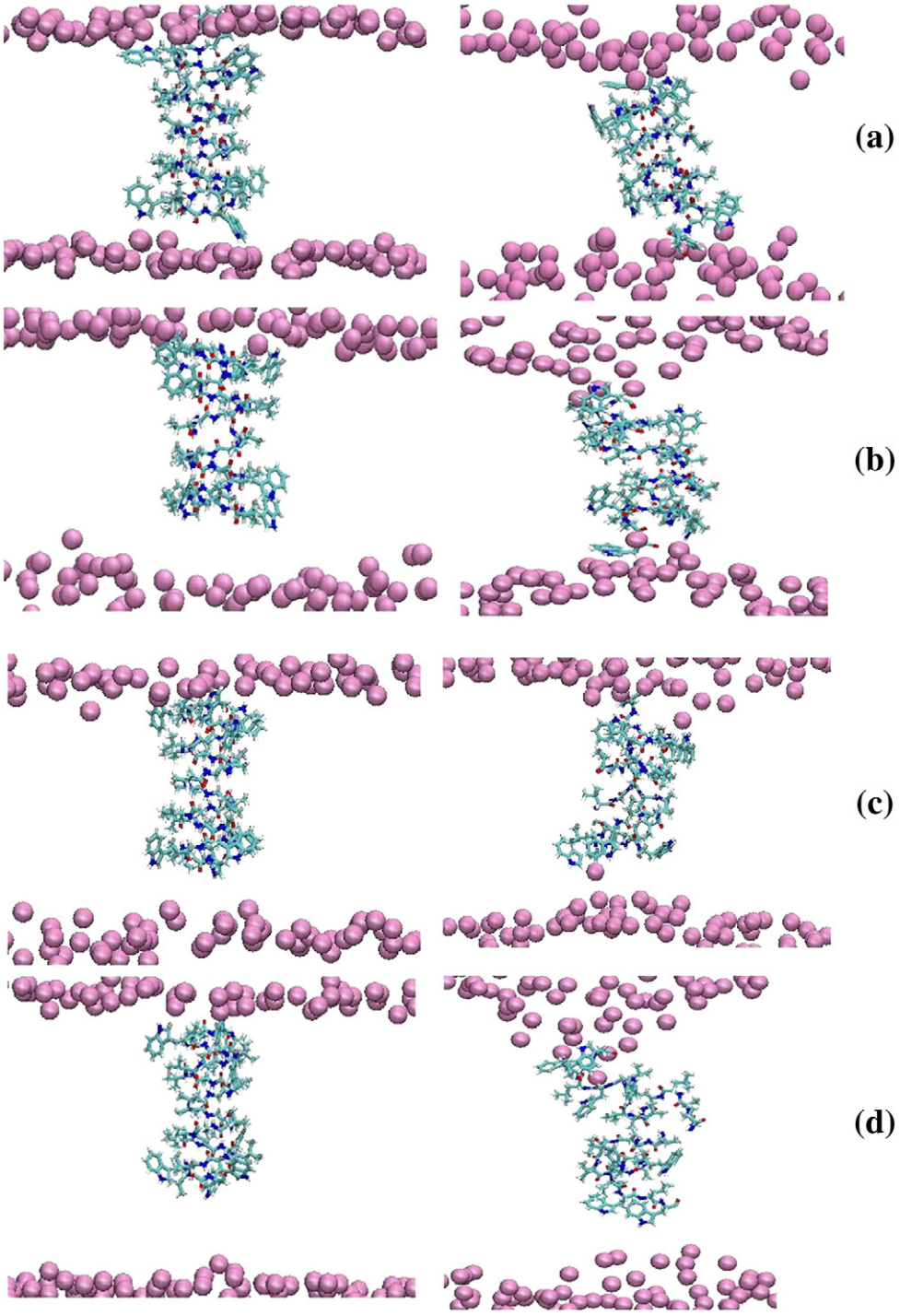

Fig. 1. The snapshots showing the gA in the bilayer after the minimization (left) and from the 100 ns time point (right). (a) → (d) represent DLPC, DMPC, POPC & DAPC systems respectively. The Phosphorus atoms of phosphate group of lipids are shown as mauve spheres. Gramicidin A is highlighted in bonds. The image rendering is done with VMD.

Time evolution of hydrophobic thickness of local and bulk lipids is shown in Fig. 2(a to d). In DLPC bilayer, the hydrophobic length of lipids is lowest among the four systems. Here the mismatch is least. After equilibration when all the constraints are removed from the system, the local lipids started to increase its hydrophobic length for better matching with that of the peptide and reached to a value almost nearly equal to that of the bulk lipids i.e. a near perfect hydrophobic adaptation between gA and the surrounding lipids was achieved in the DLPC/gA system. In case of DAPC bilayer, where there is maximum mismatch, and the lengths of the local and bulk lipids are maximum, the local lipids initially adjusted themselves with the protein by lowering the hydrophobic length by almost 9 Å from the bulk lipids and then remained almost constant. As the lipid hydrophobic thickness is much higher for DAPC compared to gA, the local lipids try to increase its length to match with that of the protein and the extent of increment is highest here. For POPC, the difference between the lengths of local and bulk lipids remains almost constant, where the difference between the local and bulk lipids is slightly increased in DMPC. The average local lipid hydrophobic thickness of DMPC bilayer is 3.5 Å greater than that of DLPC which is comparable with the previous finding that the local

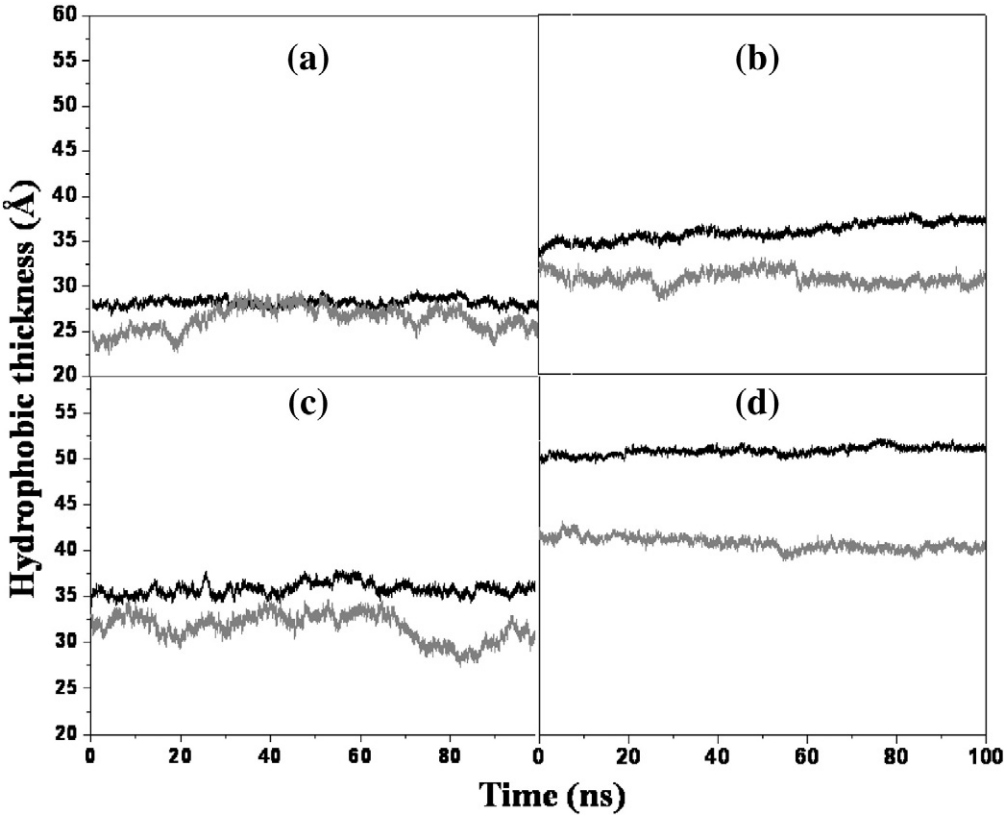

Fig. 2. Hydrophobic widths for both bulk (black line) and local (grey line) lipids as a function of time in (a) DLPC, (b) DMPC, (c) POPC, and (d) DAPC. The calculation was done from the 100 ns simulation trajectory after the equilibration.

thickness of DMPC is 2 Å higher than DLPC [42]. The observed membrane thickness is comparable with the experimental bilayer thickness [43]. Although we used a lower protein/lipid ratio (1:124), our results agree well with those studies which are done using a higher peptide/lipid ratio [44,45]. The difference in the behaviour of the local and bulk lipids in different systems is likely to originate due to the local lipid adaptations to overcome the mismatch.

To verify the extent of alteration in the local lipid structure and dynamics due to hydrophobic mismatch, we have calculated the area per lipid, area compressibility modulus (Table 1), and lipid tail order parameters (Fig. S1 of the Supporting Information) for the local and bulk lipids separately. Local lipid disorder was observed in all the systems with almost similar structural properties. In DLPC with the most matching situation, the difference in order parameters between the local and bulk lipids is least. For the other three systems the local lipids adjusted their lengths by disordering their acyl tails so the order parameter became smaller. Our results are in agreement with the experimental works by Cornell et al. [44,46] where a disorder in lipid bilayer in the presence of Gramicidin A was reported. The properties of the bulk and local lipids of DLPC, DMPC and POPC bilayer match well with previous findings [30]. We found that the area per bulk lipid values are 61.06, 56.66 and 65.55 in $Å^2$ for DLPC, DMPC and POPC respectively which agree well with the previous studies [47–49]. Local lipid head group area is higher in each case as in accordance with the previous studies [24]. Local lipid thinning observed is also comparable with earlier data [3,19,24,50]. The area compressibility modulus obtained for the systems indicates that the local lipids are more deformed than the bulk in accordance with the order parameter values [51]. A control simulation of pure DAPC bilayer consisted of 128 lipids was done and area per lipid, hydrophobic thickness and order parameter were calculated (Figs. S2, S3, S4 of the Supporting Information). These values are in good correlation with that of the bulk lipids in the gA/DAPC system.

Table 1
Membrane properties.

System	Area per lipid ($Å^2$)		Area-compressibility modulus (dyn/cm)	
	Local	Bulk	Local	Bulk
DLPC/gA	64.9 ± 2.5	61.09 ± 0.95	183 ± 10	434 ± 6.9
DMPC/gA	58.22 ± 2.5	56.32 ± 1.06	146 ± 8	320 ± 6.2
POPC/gA	70.09 ± 2.5	65.55 ± 1.2	159 ± 9.5	289 ± 6
DAPC/gA	53.04 ± 1.8	49.60 ± 0.4	267 ± 11	1955 ± 16

Any heavy atom of a lipid that lies within 5 Å from any backbone atom of the peptide is defined as local lipid and the rest are bulk lipids.
Area compressibility modulus is defined by the equation [79]:

$$K_A = \frac{\kappa_B T A_0}{N(\delta A_0^2)}$$

where A_0 is the area per lipid, δA_0 is the root mean square fluctuation of the area per lipid and N is the number of lipid per leaflet of the bilayer.

3.2. Peptide adaptations

Gramicidin A is very sensitive to external environment and may change its conformation depending upon the nature of the peripheral medium [15]. Peptide adaptations in hydrophobic mismatch are discussed below:

3.2.1. Peptide tilting

One major response to hydrophobic mismatch is peptide tilting. The tilt angle is defined as the angle formed by the peptide helical axis with the membrane normal. In case of negative hydrophobic mismatch, peptide tilting is not a very prominent response and it has been reported

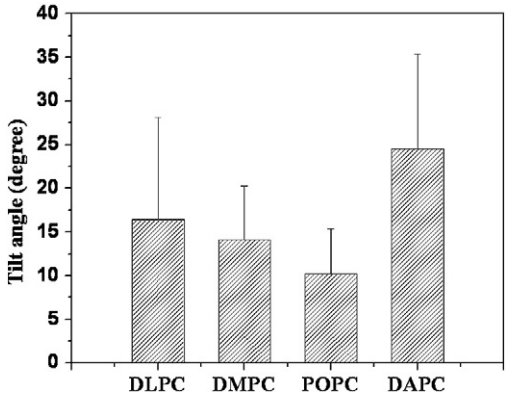

Fig. 3. Time average tilt angle of the protein for all the four systems.

that tilting up to 10° is inherent in negative mismatch [3]. In all the four systems, the peptide exhibits a small tilt angle ranging from 10° to 24° (Fig. 3). This is well correlated with the experimental work of gA in DMPC membrane [52]. As the length increases from DLPC to POPC (i.e. the extent of negative mismatch increases), the tilt angle decreases from 16.4° in DLPC to 10.22° in POPC bilayer with the exception in DAPC bilayer i.e. to maximize the extent of hydrophobic matching tilt angle decreases with the increase of lipid hydrophobic thickness [53].

3.2.2. Peptide effective hydrophobic length

For a more focused assessment of peptide response to hydrophobic mismatch, we plot peptide effective hydrophobic length as a function of time (Fig. 4). In principle, besides tilting, the peptide under mismatch could also change their effective length by a change in conformation i.e. by distorting the backbone configuration from the original one. In the channel form, the four tryptophan residues at the C terminus occupy the interfacial location of membrane which helps gA to retain its channel activity. It was observed that with replacement of tryptophan with other aromatic side chains such as phenylalanine or tyrosine, the anti-parallel double helical non-channel conformation becomes the most preferred conformation [54,55]. Thus, to determine the preferred conformer, the interfacial localization of tryptophan and their preferential side chain orientations in membranes is required [56]. Unlike positive mismatch, in the present simulations, all hydrophobic residues are placed in a hydrophobic region, so the observed distortion arises due to unfavourable positioning of tryptophan residues and there is a high possibility of tryptophan snorkelling toward the interface to gain the preferred location [57]. Due to tryptophan snorkelling toward the interface, the peptide becomes stretched and thus, the effective hydrophobic length of the peptide is greater in negative mismatch than the original one. In DAPC, as the lipid hydrophobic thickness is highest, the tryptophan 15 residue in monomer 1 which is located at the membrane hydrophobic core, has to cover more distance to reach the interface. So we expect the effective hydrophobic length should be highest in DAPC. However, as depicted from Fig. 4, the length is highest for POPC. To explain this, if we look at the membrane properties of the local lipid plot of DAPC and POPC bilayers, we can obviously detect that the trend of local lipids in the case of DAPC is more adjusting than that of POPC (in DAPC, the hydrophobic thickness of the local lipids decreases, but in POPC it remains almost constant). It indicates that in POPC bilayer local lipid adaptation is smaller which may be due to the presence of unsaturation in the acyl tail. To elucidate the effect of the presence of unsaturation, we have calculated the number of contacts of the protein with the two acyl chains of lipid (named as C2 and C3 where C2 is the unsaturated tail of POPC) within 4 Å individually in Table S2. It is seen that in DLPC, DMPC and DAPC where both the tails are fully saturated, they contributed equally, but in POPC the saturated tails take part almost double in contribution than that of the unsaturated tail. So it may be the reason that the protein in POPC increases its length more to maximize the number of favourable contacts instead of local lipid adjustment. For DLPC and DMPC systems, the effective hydrophobic thickness are smaller than the other two systems and the values are nearly equal to the value of effective hydrophobic thickness of the functional Gramicidin A dimer (22 Å) [20] which explains the preservation of channel conformation in DLPC and DMPC systems.

The lipid adjustment plot (Fig. 5) authenticates the above justification about the highest length of the peptide in POPC bilayer. We have defined lipid adjustment (ΔL) as the difference between the hydrophobic length of local and bulk lipids respectively. For negative mismatch ΔL is negative. Here we observe that lipid adjustment is smaller in POPC than in DMPC and DAPC. For DAPC it is mostly negative and slightly increasing in value, it is also increasing in value in the case of DMPC. It indicates that in DAPC, ΔL is highest which is comprehensible as the length of the local lipids is reducing, increasing the difference between the length of the bulk and local lipids. For DLPC, it is initially negative but then reaches to almost zero as here the local lipid thickness

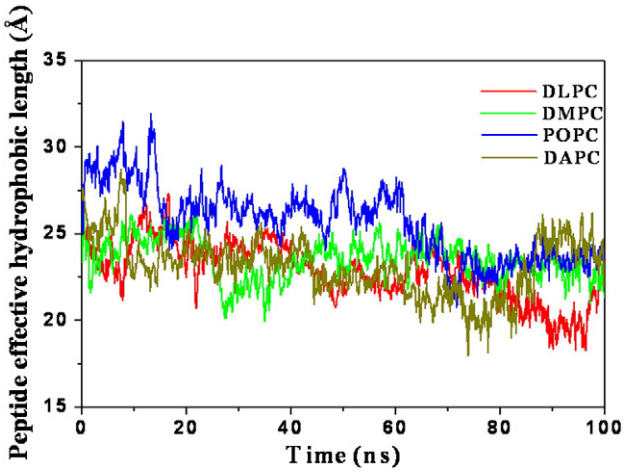

Fig. 4. Time evolution of peptide effective hydrophobic length for the four systems. Blue line for POPC, green for DMPC, dark yellow for DAPC and red line represents DLPC system. The effective hydrophobic length of peptide is defined as: $L^{eff} = (L^{TM})\cos\theta$ where θ the dimer tilt angle and L^{TM} is the peptide end to end distance with respect to time.

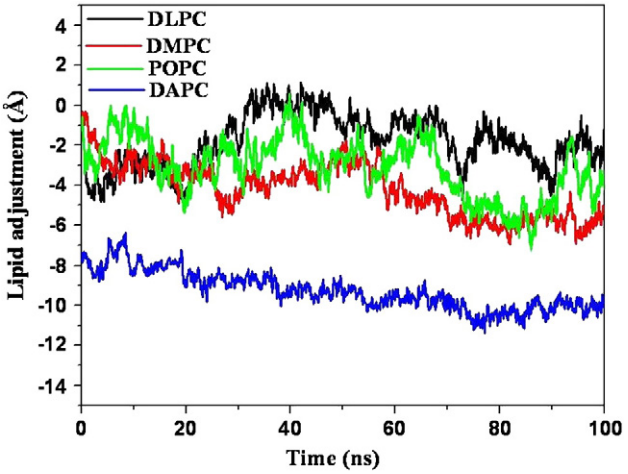

Fig. 5. Local lipid adjustment ($\Delta L^{adaptation}$) as a function of time in gA/DLPC (black line), gA/DMPC (red line), gA/POPC (green line), and gA/DAPC (blue line) systems: $\Delta L^{adaptation} = (L^{contact} - L^{bulk})$, where $L^{contact}$ and L^{bulk} are the hydrophobic thickness of contact and bulk lipids respectively.

increases initially and ultimately reaches to the similar value of the bulk lipids.

3.2.3. Gramicidin A secondary structure

One alternative mechanism to overcome the hydrophobic mismatch is for the protein to change its secondary structure or undergo some conformational changes. The specific conformational drift was obtained by computing the root mean square deviation (RMSD) of protein backbone relative to its starting structure (Fig. 6a). In the DLPC/gA system, it is lowest and after an initial increase it converges to a value nearly equal to 2 Å which indicates its conformational stability in the DLPC bilayer. For DMPC bilayer, it is also small (3 Å) signifying stability with little structural fluctuation in the bilayer. In POPC, it is ≈4 Å which is relatively higher than in DLPC and DMPC, but smaller than in DAPC. In DAPC, gA conformation deviates significantly from its initial structure as reflected from a high RMSD value of 6.5 Å. This designates the conformational stability of gA in DLPC, in DMPC and also in POPC and instability in DAPC (also observed from Fig. 1). As we started with the head to head dimer $\beta^{6.3}$ helix which is proved to be the channel conformation and this structure is stable in DLPC, DMPC and almost in POPC, we can expect that gA retains its channel activity in DLPC, DMPC and POPC bilayers [19,58]. The structure and conformation in DMPC system remained almost the same as reported earlier [59,60]. The dimer stability is again confirmed by the total number of hydrogen bonds in gA (Fig. S5 of the Supporting Information). The probability plot of the total number of hydrogen bonds demonstrates that the number is reduced from 25 to 11 in DLPC to DAPC which signifies that the channel structure is lost in DAPC.

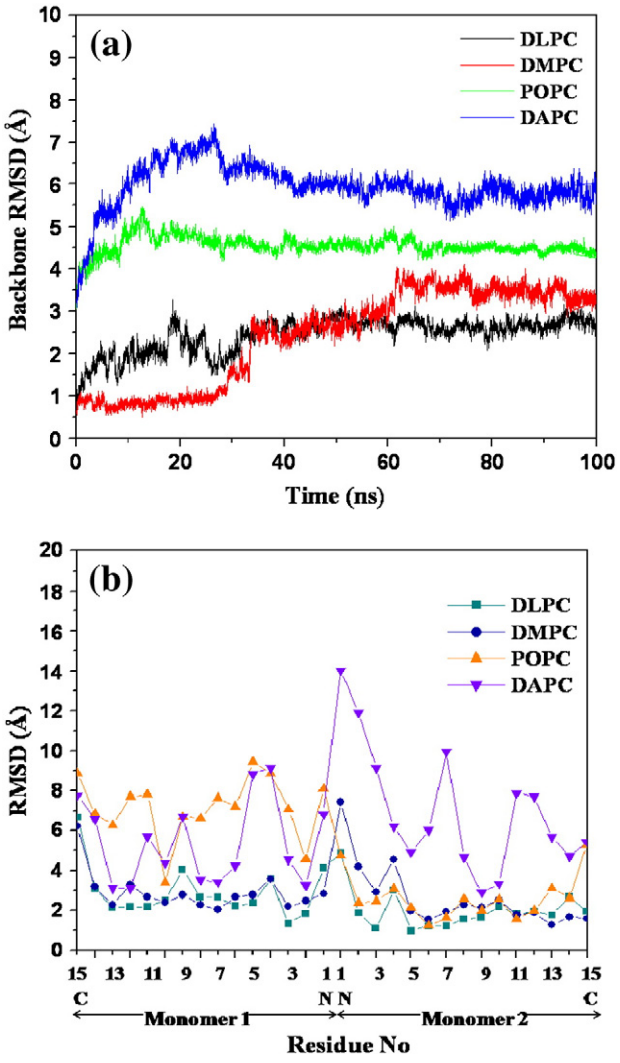

Fig. 6. (a) The RMSD from the initial point for the protein backbone as a function of the simulation time. (b) The time average RMSD value of the individual residues of the protein.

For a more detailed understanding, residue based RMSD analysis (Fig. 6b) shows stable value for all the residues in the case of DLPC and DMPC except for the terminal residues. In all four cases, the C terminal tryptophan (Trp15) of the 2nd monomer which is located at the interface shows a lesser value than Trp15 of other monomer (which is located away from the interface). In POPC, the residues of the 1st monomer (residues 1–15) show a larger RMSD value than that of DAPC, but for the 2nd monomer it is just reversed where the RMSD values of individual residues are higher in the case of DAPC bilayer than that of in POPC. Also the N terminal residues of the 2nd monomer (Val1, Gly2) show a large RMSD value in DAPC bilayer where for the rest three systems these residues show low fluctuation. As the protein in POPC bilayer stretches its length to overcome the mismatch, the residues of the protein have to fluctuate from its original position. So the large fluctuation of residues 1 to 15 of the 1st monomer in POPC than in the other systems and the reason behind the highest effective hydrophobic thickness of the protein can be correlated. The 2nd monomer in DAPC shows a larger deviation which is discussed next.

To characterize the peptide orientation and to explain better the root mean square deviation of individual residues, the average z position (for the final 10 ns of simulation trajectory) of the individual residues of gA was plotted and compared with the initial orientation with respect to the bilayer interface (Fig. 7). It has been reported that the interfacial localization of the tryptophan residues is a compulsory feature of gramicidin channel conformation and function in membranes [9]. So we placed gA in a bilayer such as C terminal tryptophan residues of one monomeric subunit (monomer 2) could be placed at the hydrophobic/hydrophilic interface and it is visible from the plot that initially Trp15 residue of the 2nd monomer is located near the bilayer interface (2–3.5 Å under the phosphate plane). This places the other C terminal end tryptophan15 residue almost near the other interface (3.0 Å under the phosphate plane) in the case of DLPC bilayer (Fig. 7b) as its hydrophobic width is nearly matching with that of the gA. As shown in Fig. 7d, Trp-15 in monomer 1 is just below the interface for DMPC and POPC. But in DAPC bilayer with larger thickness, gA is approximately 10 Å away from the interface (Fig. 7f, h). So in DAPC, Trp-15 resides at the hydrophobic core and this unfavourable positioning forces gA to modify its position. The plots for the final 10 ns trajectory indicates that in DMPC and DAPC (and to some extent in DLPC), the peptide allows itself to move to the other interface (described as UP_P), but in POPC, the tryptophan15 residue of monomer 2 remains stable at the interface throughout the simulation, this is again confirmed by the total number of hydrogen bonds of this residue with the lipid head group (phosphate and carbonyl oxygen) shown in Table 2. But to compensate the imposed mismatch and to place the other C terminal Trp15 residue at the interface region (UP_P), in POPC bilayer, gA increases its length rather than moving like in DMPC or DAPC resulting in large RMSD of monomer 1 (Fig. 6b) thereby achieving the highest effective hydrophobic length (Fig. 4). In DAPC bilayer as the protein itself moves to another interface to place its tryptophan residues at the favourable position, the higher RMSD for the 2nd monomer can be attributed to this.

Another important observation from the above plot (Fig. 7) is that the N-N distance of the head to head dimer has been increased from that of the initial structure which may indicate the alteration from a channel to non-channel conformer. Initially it was ~1.3 Å, but it changes to ~4 Å in DAPC, for DLPC and DMPC this value is almost constant just by increasing ~1 Å. This increment is slightly higher in POPC than that of DLPC and DMPC. An increase of 4 Å in DAPC seems not to be a very

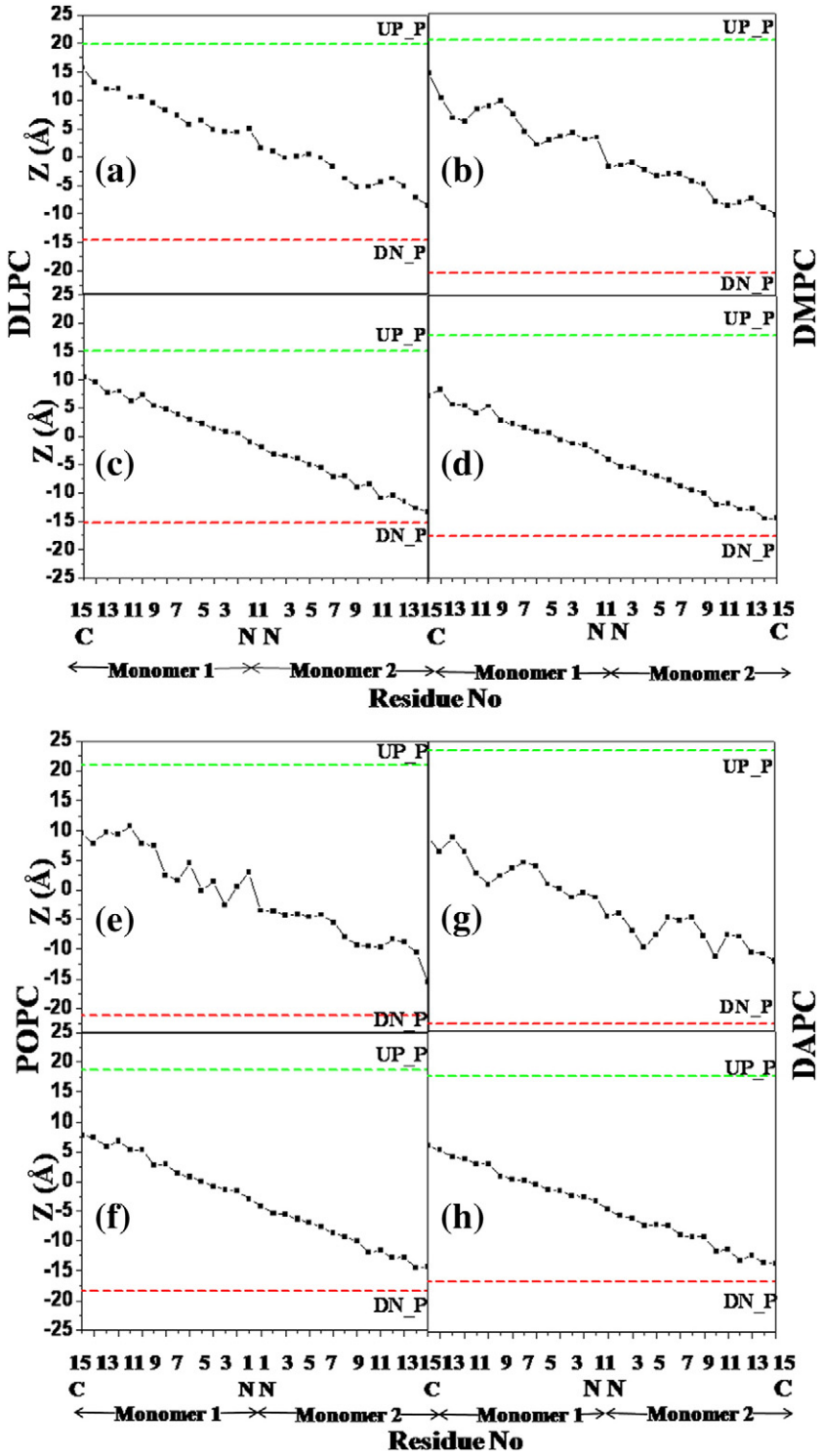

Fig. 7. Z-coordinate of the average position of centre of mass of the individual residues (black), the average position of centre of mass of PO_4 head group in the upper (green dotted line, defined by UP_P) and in the lower layer (red dotted line, defined by DN_P) respectively obtained upon averaging over the last 10 ns of the simulation trajectory(subpanels: a, c, e, and g for DLPC, DMPC, POPC, and DAPC respectively) and the starting structure after minimization (subpanels: b, d, f, and h for DLPC, DMPC, POPC, and DAPC respectively).

Table 3
Hydrogen bond occupancy at the monomeric interface of the gA dimer.

	DLPC	DMPC	POPC	DAPC
H-bond occupancy (%)	99.18	64.3	10.75	0.0

The occupancy is the percentage of keeping hydrogen bond throughout the simulation time.

prominent inspection from the channel to non channel conversation, so there may be some other conformational changes in the gA dimer in DAPC. So we have plotted the interhelical angle (θ) between the two monomers (Fig. 8) and found that for DAPC, most of the time this adopts an angle ~90° i.e. one monomer is remained almost perpendicular with respect to another. Whereas for DMPC, POPC and DLPC, the corresponding values are 140 ± 30°, 140 ± 25° and 160 ± 20°

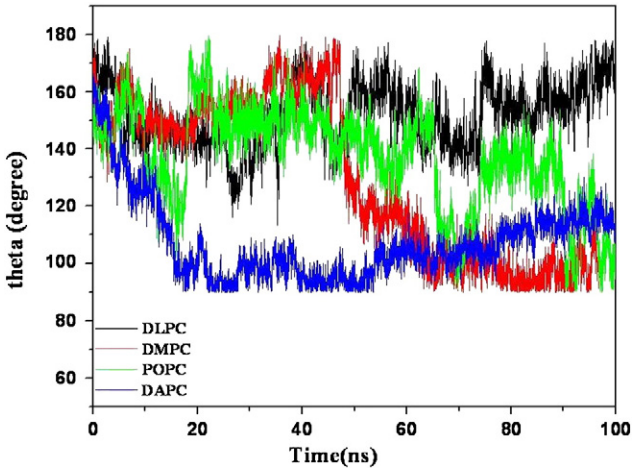

Fig. 8. The interhelical angle (θ) between the two monomers of Gramicidin A as a function of time in DLPC (black), DMPC (red), POPC (green), and DAPC (blue). The angle is defined as the angle created by the two connecting axes of the two monomers where the axis is formed by joining the centre of masses of the N and C terminal residues.

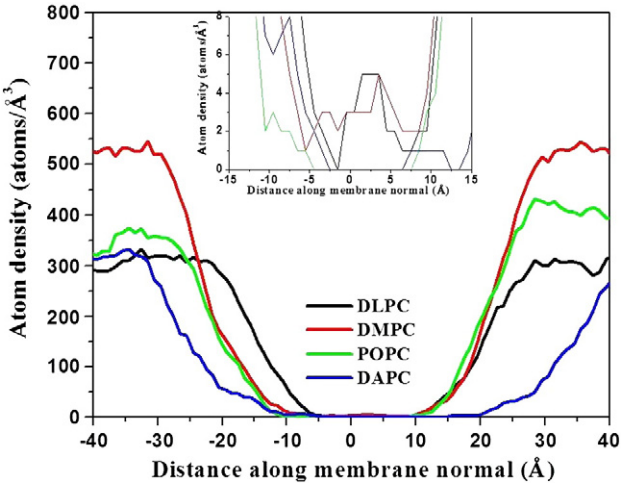

Fig. 9. The atom density distributions of oxygen atoms of water molecules for the four protein/bilayer systems (averaged over the last 10 ns of the simulation trajectory). Water penetration in the membrane centre in DLPC (black line) and in DMPC (red line) is visualized from the inset of this figure.

respectively although the value decreases at some stages of the simulation for POPC and DMPC [52], but most of the time they show a value very close to the initial structure i.e. almost parallel orientation. Again the higher RMSD value of the N terminal residues of the 2nd monomer in DAPC (Fig. 6b) can be ascribed from this analysis as here the monomers are tilted with respect to each other, they had to undergo through more structural deviations than in the other systems.

Gramicidin channel gating is known to occur by a well defined conformational change through the formation and dissociation of the transmembrane dimer [61]. Breaking of hydrogen bonds at the monomer interface and lateral movement of the monomers are involved in conformational changes [62]. To prove the above finding in our case we have calculated the percentage of H-bond occupancy at the monomer interface of the dimer in the four systems (Table 3) and find that it decreases from DLPC to POPC and almost become zero in the DAPC/gA system suggesting conformational change in the last system. Moreover we find that the effective hydrophobic thickness of gA increases in the POPC and DAPC systems, and it has been shown experimentally that when gramicidin analogues of reduced lengths are used, the channel activity is enhanced in lipid membrane [63]. So increment in hydrophobic length is also significant for conversion to a non-channel structure. In addition we have also observed lateral movement of gA monomer in DAPC. Taking all the above findings together, it can be concluded that in DAPC, the channel conformer of Gramicidin A is more or less converted to the non-channel conformer while in POPC, it retains its channel structure with little fluctuations and in DLPC and DMPC the channel structure is entirely intact.

3.3. Channel activity in membranes

From the previous analysis, we noticed that in DAPC the channel conformation of the head to head $\beta^{6,3}$ helix of Gramicidin A is not retained. As the channel conformer of gA is known to permeate monovalent cation along with water [64], we have calculated the atom density distribution of water molecules along the Z axis (i.e. the membrane normal) for the last 10 ns simulation trajectory for the four systems. The extent of penetration can be visualized from the plot (Fig. 9). If the channel activity is intact then the channel should allow some water molecules in it. At the central region of the membrane (from Z = −10 to Z = 10), the water density is practically nil in DAPC, but for DLPC and DMPC, the value varies from 4 to 5 (Inset of Fig. 9) indicating the presence of water penetration through the channel. The water occupancy in the ion channel in the two systems can be evaluated from the number of penetrating water molecules in the channel pore with time plot for DLPC and DMPC (Fig. 10a) and it reveals that on average 10 and 15 water molecules reside in the ion channel pore. This analysis provides extra support to our observation that whether the channel structure is intact in DLPC and DMPC, it is no more retained in the DAPC system.

An interesting finding is that the Gramicidin A channel shares important structural features with ion channels [9,65]. It is established that gA forms transmembrane pores in lipid bilayers through which monovalent ion passes. Sodium ion was passed through the channel pore to observe which residues are responsible for ion binding [66,67]. The gramicidin channels and Kcsa K^+ [68] are lined by the polar carbonyl groups of the peptide backbone and ion selectivity arises due to backbone interaction with ion [3,69]. Our previous analyses suggested that the gA as well as the lipid bilayer are least perturbed in DLPC and in agreement we find that a K^+ ion enters into the channel and remained stable inside the channel throughout the simulation (Fig. 10b) due to the favourable electrostatic interaction with the hydrophilic pore formed by the carbonyl moiety (Fig. S6 in the Supporting Information). Previously we find water molecules inside the channel in DLPC and DMPC systems; here we also observe a monovalent cation inside the channel in the DLPC system that is indicative of the strong preservation of the ion channel.

Table 2
Average number of hydrogen bonds formed between tryptophan 15 of the 2nd monomer residue and the corresponding interface throughout the simulation.

	DLPC	DMPC	POPC	DAPC
No. of H-bonds	0.375	0.098	0.556	0.170

3.4. Peptide–lipid interaction

We have also calculated the interaction energies of gA with surrounding lipid molecules and partitioned the total interaction energy into electrostatic and van der Waals (vdW) terms (Fig. S7 of the Supporting Information) [70]. The plot shows that though the interaction energy is originated from both van der Waals and electrostatic interactions, vdW contribution is more. To illuminate the source of the vdW interaction, the average number of acyl group heavy atoms of lipids within 4 Å of gA heavy atoms was calculated

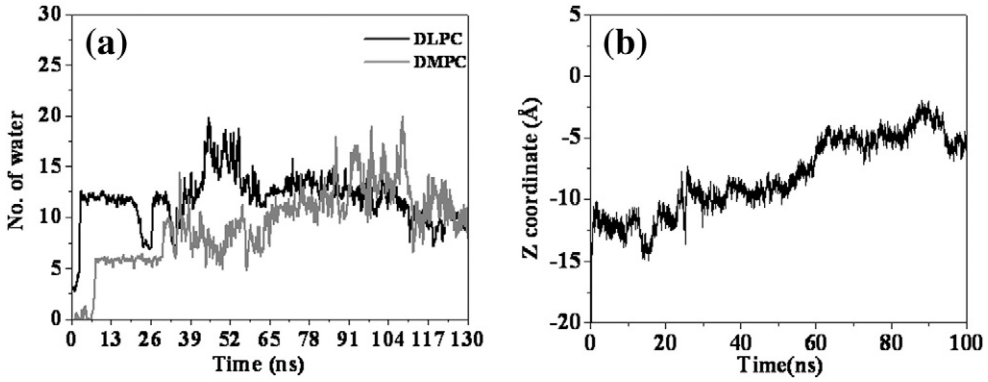

Fig. 10. (a) Number of penetrating water molecules inside the Gramicidin A channel as a function of time (Black for DLPC and grey for DMPC). (b) Time profile of z-coordinate of potassium ion penetrating in the ion channel in DLPC/gA system.

(Fig. S8 in the Supporting Information). It can be seen from the plot that the number of contacts of gA with the lipid bilayer increases from DLPC to DAPC as the number of CH2 groups in the acyl tail increases from DLPC to DAPC.

3.5. Tryptophan–tryptophan interaction in Gramicidin A

An interaction between the Trp-9 and Trp-15 indole groups is possible due to their close proximity in space in the $\beta^{6.3}$ helix conformation [9]. NMR study has shown that in sodium dodecyl sulphate (SDS) micelle Trp-9 and Trp-15 do not interact through space [71] while in DMPC bilayer they are stacked [72]. In previous experimental studies tryptophan orientation in membrane was determined and it was shown that the indole ring is oriented parallel with the channel axis [73,74]. In addition, the presence of aromatic interaction in membrane on a nanosecond timescale has been proved [75]. To explore this, we have calculated the probability distribution of angle between the indole rings of Trp-9 and Trp-15 in the two monomers separately and the average distance between the two rings in Figs. S9 and S10 respectively. We found from the distribution plot that in monomer 2 where Trp-15 is positioned at the interface, the peak locates at $\approx 0°$ i.e. Trp-9 is oriented almost parallel with Trp-15 only in the case of the DMPC system. Whereas in monomer 1, the peak in the DLPC system is located nearly at 150° i.e. it remains more or less parallel. The distance between Trp-9 and Trp-15 in monomer 2 is lower than that of the monomer 1 except for POPC. The distance is below or equal to 5 Å in DLPC and DMPC. So there is a little probability of a presence of stacking interaction in DLPC and in DMPC and as we found in our simulations on the stability of the channel conformer in the DLPC and DMPC membranes, we can conclude that stacking between Trp-9 and Trp-15 may be present in the case of channel conformer but it may not be an essential condition for the channel activity as we did not find very strong interaction. So it can be confirmed that stacking between Trp-9 and Trp-15 is not completely related to the conformation of Gramicidin A, and it depends on other factors too such as on the specific lipid environment [76], curvature of the host assembly [77] etc.

4. Conclusions

We have performed a systematic study of Gramicidin A in four different lipid bilayers which focuses on the conformational stability of Gramicidin A in different mismatched conditions. Here the simulations cover a range of mismatch situations, from nearly matching to extremely negative; with major emphasis on negative mismatch — as gA channel activity has been known to be lost in thicker lipid membranes. It was observed that the compensation of mismatch was achieved by local bilayer thinning which is reminiscent of many previous studies. Tryptophan snorkelling toward the hydrophobic/hydrophilic interface leads to increase in effective peptide length. Especially in DAPC, local bilayer thinning is not sufficient to overcome the unstable mismatched situation; here the protein itself undergoes some structural transitions to get rid of the incompatible circumstances. Also in POPC, the protein adjusted itself to overcome the mismatch. Two mechanisms in two different environments (in the presence and absence of unsaturation) were observed from our simulation, in the case of DAPC bilayer, the peptide allows itself to move to the opposite interface for positioning the tryptophan at the preferred location, whereas for in POPC, one C terminal tryptophan being stable in the interface stretches its length rather than moving to balance the energetically stressed mismatch situation. And that's why the channel activity is sharply reduced in the DAPC while under the near matching condition (in DLPC and in DMPC systems), gA retains its channel activity, by allowing water penetration inside the channel. Moreover in DLPC, gA allows a K^+ ion inside the channel. Unlike many previous simulation studies where the head to head $\beta^{6.3}$ helix conformer of gA was found to be stable in bilayers and where we find that hydrophobic mismatch does not alter gA structure, our results collectively demonstrate that channel activity of Gramicidin A is directly dependent upon the membrane thickness. It is also established that the non-channel double helix form is not the native form in lipid bilayers [78]. We are able to capture the structural transitions from a channel to non channel conformation just by placing gA in an extremely adverse environment. In spite of the fact that the channel conformer is thermodynamically more stable, we can shed light to the fact that it can convert to a state without channel activity under extreme negative mismatch circumstance. Moreover, here we have used the DAPC lipid bilayer in gel phase which motivates us to study the DAPC lipid bilayer in fluid phase which will be really interesting.

Acknowledgements

This work is partially supported by the Department of Science and Technology, Government of India, [Project number: No. SR/S1/PC-60/2009] and a fellowship to IB through UGC-NET. We are also thankful to the NANO Project (CONV/002/NANORAC/2008) of the Department of Chemistry, University of Calcutta, Kolkata, India and to the RCAMOS of the Indian Association for the Cultivation of Science, Kolkata, India, for providing the "High Performance Computing" facility.

Appendix A. Supplementary data

Supporting information. Data regarding the equilibration of pure POPC bilayer, the order parameter profile for the four systems,

interaction energy diagram, calculation of number of hydrogen bonds and the contacts of the protein with membranes, probability distribution of inter-dimer hydrogen bonds of Gramicidin A plots and the plots of distance and angle between Trp-15 and Trp-9 are given along with the table showing the no of contacts of gA with lipid C2 and C3 acyl tails separately. Supplementary data to this article can be found online at http://dx.doi.org/10.1016/j.bbamem.2013.10.005.

References

[1] M.O. Jensen, O.G. Mouritsen, Lipids do influence protein function—the hydrophobic matching hypothesis revisited, Biochim. Biophys. Acta 1666 (2004) 205–226.
[2] O.S. Anderson, R.E. Koppe, Bilayer thickness and membrane protein function: an energetic perspective, Annu. Rev. Biophys. Biomol. Struct. 36 (2007) 107–130.
[3] S.K. Kandasamy, R.G. Larson, Molecular dynamics simulations of model trans-membrane peptides in lipid bilayers: a systematic investigation of hydrophobic mismatch, Biophys. J. 90 (2006) 2326–2343.
[4] F. Yin, J.T. Kindt, Atomistic simulation of hydrophobic matching effects on lipid composition near a helical peptide embedded in mixed-lipid bilayers, J. Phys. Chem. B 114 (2010) 8076–8080.
[5] D.L. Parton, J.W. Klingelhoefer, M.S.P. Sansom, Aggregation of model membrane proteins, modulated by hydrophobic mismatch, membrane curvature, and protein class, Biophys. J. 101 (2011) 691–699.
[6] S.B. Hladky, D.A. Haydon, Ion transfer across lipid membranes in the presence of gramicidin A: I. Studies of the unit conductance channel, Biochim. Biophys. Acta 274 (1972) 294–312.
[7] F.M. Harold, J.R. Baarda, Gramicidin, valinomycin, and cation permeability of *Streptococcus faecalis*, J. Bacteriol. 94 (1967) 53–60.
[8] B. Cornell, Gramicidin A-phospholipid model systems, J. Bioenerg. Biomembr. 19 (1987) 655–676.
[9] D.A. Kelkar, A. Chattopadhyay, The gramicidin ion channel: a model membrane protein, Biochim. Biophys. Acta 1768 (2007) 2011–2025.
[10] R. Sarges, B. Witkop, A.V. Gramicidin, The structure of valine- and isoleucine-gramicidin A, J. Am. Chem. Soc. 87 (1965) 2011–2020.
[11] J.B.O. Mitchell, J.D. Smith, D-amino acid residues in peptides and proteins, Proteins 50 (2003) 563–571.
[12] J.P. Segrest, R.J. Feldmann, Membrane proteins: amino acid sequence and membrane penetration, J. Mol. Biol. 87 (1974) 853–858.
[13] D.W. Urry, The gramicidin A transmembrane channel: a proposed 7r (L, D) helix, Proc. Natl. Acad. Sci. 68 (1971) 672–676.
[14] W.R. Veatch, E.T. Fossel, E.R. Blout, Conformation of gramicidin A, Biochemistry 13 (1974) 5249–5256.
[15] S. Bransburg-Zabary, A. Kessel, M. Gutman, N. Ben-Tal, Stability of an ion channel in lipid bilayers: implicit solvent model calculations with gramicidin, Biochemistry 41 (2002) 6946–6954.
[16] J.A. Killian, K.U. Prasad, D. Hains, D.W. Urry, The membrane as an environment of minimal interconversion. A circular dichroism study on the solvent dependence of the conformational behavior of gramicidin in diacylphosphatidylcholine model membranes, Biochemistry 27 (1988) 4848–4855.
[17] S.V. Sychev, L.I. Barsukov, V.T. Ivanov, The double ππ5.6 helix of gramicidin A predominates in unsaturated lipid membranes, Eur. Biophys. J. 22 (1993) 279–288.
[18] M. Zein, R. Winter, Effect of temperature, pressure and lipid acyl chain length on the structure and phase behaviour of phospholipid–gramicidin bilayers, Phys. Chem. Chem. Phys. 2 (2000) 4545–4551.
[19] D.A. Kelkar, A. Chattopadhyay, Modulation of gramicidin channel conformation and organization by hydrophobic mismatch in saturated phosphatidylcholine bilayers, Biochim. Biophys. Acta 1768 (2007) 1103–1113.
[20] J.R. Elliott, D. Needham, J.P. Dilger, D.A. Haydon, The effects of bilayer thickness and tension on gramicidin single-channel lifetime, Biochim. Biophys. Acta 735 (1983) 95–103.
[21] A.J. de Jesus, T.W. Allen, The determinants of hydrophobic mismatch response for transmembrane helices, Biochim. Biophys. Acta 1828 (2013) 851–863.
[22] E. Strandberg, S. Esteban-Martin, A.S. Ulrich, J. Salgado, Hydrophobic mismatch of mobile transmembrane helices: merging theory and experiments, Biochim. Biophys. Acta 1818 (2012) 1242–1249.
[23] J. Yoo, Q. Cui, Three-dimensional stress field around a membrane protein: atomistic and coarse-grained simulation analysis of gramicidin A, Biophys. J. 8 (2013) 117–127.
[24] T. Kim, K.I. Lee, P. Morris, R.W. Pastor, O.S. Andersen, W. Im, Influence of hydrophobic mismatch on structures and dynamics of gramicidin A and lipid bilayers, Biophys. J. 102 (2012) 1551–1560.
[25] B.A. Cornell, F. Separovic, D.E. Thomas, A.R. Atkins, R. Smith, Effect of acyl chain length on the structure and motion of gramicidin A in lipid bilayers, Biochim. Biophys. Acta 985 (1989) 229–232.
[26] N. Mobashery, C. Nielsen, O.S. Andersen, The conformational preference of gramicidin channels is a function of lipid bilayer thickness, FEBS Lett. 412 (1997) 15–20.
[27] J.C. Phillips, R. Braun, W. Wang, J. Gumbart, E. Tajkhorshid, E. Villa, C. Chipot, R.D. Skeel, L. Kale, K. Schulten, Scalable molecular dynamics with NAMD, J. Comp. Chem. Soc. 26 (2005) 1781–1802.
[28] A.D. Mackerell Jr., D. Bashford, M. Bellott, R.L. Dunbrack Jr., J.D. Evanseck, M.J. Field, S. Fischer, J. Gao, H. Guo, S. Ha, D. Joseph-McCarthy, L. Kuchnir, K. Kuczera, F.T.K. Lau, C. Mattos, S. Michnick, T. Ngo, D.T. Nguyen, B. Prodhom, W.E. Reiher III, B. Roux, M. Schienkrich, J.C. Smith, R. Stote, J. Straub, M. Watanabe, J. Wiorkiewicz-Kuczera, D. Yin, M.J. Karplus, All-atom empirical potential for molecular modeling and dynamics studies of proteins, J. Phys. Chem. B 102 (1998) 3586–3616.
[29] A.D. Mackerell Jr., M. Feig, C.L. Brooks III, Extending the treatment of backbone energetics in protein force fields: limitations of gas-phase quantum mechanics in reproducing protein conformational distributions in molecular dynamics simulations, J. Comput. Chem. 25 (2004) 1400–1415.
[30] S. Jo, T. Kim, V.G. Iyer, W. Im, CHARMM-GUI: a web-based graphical user interface for CHARMM, J. Comput. Chem. 29 (2008) 1859–1865.
[31] W.L. Jorgensen, J. Chandrasekhar, J.D. Madura, R.W. Impey, M.L. Klein, Comparison of simple potential functions for simulating liquid water, J. Chem. Phys. 79 (1983) 926–935.
[32] R.R. Ketchem, K.C. Lee, S. Huo, T.A. Cross, Macromolecular structural elucidation with solid-state NMR-derived orientational constraints, J. Biomol. NMR 8 (1996) 1–14.
[33] R.E. Koeppe, O.S. Andersen, Engineering the gramicidin channel, Annu. Rev. Biophys. Biomol. Struct. 25 (1996) 231–258.
[34] S.E. Feller, Y. Zhang, R.W. Pastor, B.R. Brooks, Constant pressure molecular dynamics simulation: the Langevin piston method, J. Chem. Phys. 103 (1995) 4613–4621.
[35] B.J. Litman, E.N. Lewis, I.W. Levin, Packing characteristics of highly unsaturated bilayer lipids: Raman spectroscopic studies of multilamellar phosphatidylcholine dispersions, Biochemistry 30 (1991) 313–319.
[36] T. Darden, D. York, L. Pedersen, Particle mesh Ewald: an $N\cdot\log(N)$ method for Ewald sums in large systems, J. Chem. Phys. 98 (1993) 10089–10092.
[37] H.C. Anderson, Rattle: a "velocity" version of the shake algorithm for molecular dynamics calculations, J. Chem. Phys. 52 (1983) 24–34.
[38] S. Miyamoto, P.A. Kollman, Settle: an analytical version of the SHAKE and RATTLE algorithm for rigid water models, J. Comput. Chem. 13 (1992) 952–962.
[39] B.R. Brooks, R.E. Bruccoleri, B.D. Olafson, D.J. States, S. Swaminathan, M. Karplus, CHARMM: a program for macromolecular energy, minimization, and dynamics calculations, J. Comput. Chem. 4 (1983) 187–217.
[40] W. Humphrey, A. Dalke, K. Schulten, VMD: visual molecular dynamics, J. Mol. Graphics 14 (1996) 33–38.
[41] T.A. Harroun, W.T. Heller, T.M. Weiss, L. Yang, H.W. Huang, Theoretical analysis of hydrophobic matching and membrane-mediated interactions in lipid bilayers containing gramicidin, Biophys. J. 76 (1999) 937–945.
[42] W.K. Nitschke, C.C. Vequi-Suplicy, K. Coutinho, H. Stassen, Molecular dynamics investigations of PRODAN in a DLPC bilayer, J. Phys. Chem. B 116 (2012) 2713–2721.
[43] B.A. Cornell, F. Separovic, Membrane thickness and acyl chain length, Biochim. Biophys. Acta 733 (1983) 189–193.
[44] B.A. Cornell, L.E. Weir, F. Separovic, The effect of gramicidin A on phospholipid bilayers, Eur. Biophys. J. 16 (1988) 113–119.
[45] B.A. Cornell, F. Separovic, A model for gramicidin A -phospholipid interactions in bilayers, Eur. Biophys. J. 16 (1988) 299–306.
[46] L.K. Nicholson, F. Moll, T.E. Mixon, P.V. LoGrasso, J.C. Lay, T.A. Cross, Solid-state ^{15}N NMR of oriented lipid bilayer bound gramicidin A, Biochemistry 26 (1987) 6621–6626.
[47] D. Poger, A.E. Mark, On the validation of molecular dynamics simulations of saturated and *cis*-monounsaturated phosphatidylcholine lipid bilayers: a comparison with experiment, J. Chem. Theory Comput. 6 (2010) 325–336.
[48] S.A. Pandit, S.W. Chiu, E. Jakobsson, A. Grama, J.L. Scott, Cholesterol surrogates: a comparison of cholesterol and 16:0 ceramide in POPC bilayers, Biophys. J. 92 (2007) 920–927.
[49] M.-L. Ainalem, R.A. Campbell, S. Khalid, R.J. Gillams, A.R. Rennie, T. Nylander, On the ability of PAMAM dendrimers and dendrimer/DNA aggregates to penetrate POPC model biomembranes, J. Phys. Chem. B 114 (2010) 7229–7244.
[50] J.C. Mathai, S. Tristram-Nagle, J.F. Nagle, M.L. Zeidel, Structural determinants of water permeability through the lipid membrane, J. Gen. Physiol. 131 (2008) 69–76.
[51] E. Strandberg, S. Özdirekcan, D.T.S. Rijkers, P.C.A. van der Wel, R.E. Koeppe, R.M.J. Liskamp, J.A. Killian, Tilt angles of transmembrane model peptides in oriented and non-oriented lipid bilayers as determined by ^{2}H solid-state NMR, Biophys. J. 86 (2004) 3709–3721.
[52] F. Separovic, R. Pax, B.A. Cornell, NMR order parameter analysis of a peptide plane aligned in a lyotropic liquid crystal, Mol. Phys. 78 (1993) 357–369.
[53] W.M. Yau, W.C. Wimley, K. Gawrisch, S.H. White, The preference of tryptophan for membrane interfaces, Biochemistry 37 (1998) 14713–14718.
[54] M. Cotten, F. Xu, T.A. Cross, Protein stability and conformational rearrangements in lipid bilayers: linear gramicidin, a model system, Biophys. J. 73 (1997) 614–623.
[55] D. Salom, M.C. Baño, L. Braco, C. Abad, HPLC demonstrates that an all Trp → Phe replacement in gramicidin A results in a conformational rearrangement from β-helical monomer to double-stranded dimer in model membranes, Biochem. Biophys. Res. Commun. 209 (1995) 466–473.
[56] H. Sun, D.V. Greathouse, O.S. Andersen, R.E. Koeppe II, The preference of tryptophan for membrane interfaces insights from n-methylation of tryptophans in gramicidin channels, J. Biol. Chem. 283 (2008) 22233–22243.
[57] B.L. de Groot, D.P. Tieleman, P. Pohl, H. Grubmüller, Water permeation through gramicidin A: desformylation and the double helix: a molecular dynamics study, Biophys. J. 82 (2002) 2934–2942.
[58] A.M. O' Connell, R.E. Koppe II, O.S. Anderson, Kinetics of gramicidin channel formation in lipid bilayers: transmembrane monomer association, Science 250 (1990) 1256–1259.
[59] B.A. Cornell, F. Separovic, A.J. Baldassi, R. Smith, Conformation and orientation of gramicidin A in oriented phospholipid bilayers measured by solid state carbon 13 NMR, Biophys. J. 53 (1988) 67–76.

[60] R. Smith, D.E. Thomas, F. Separovic, A.R. Atkins, B.A. Cornell, Determination of the structure of a membrane-incorporated ion channel. Solid-state nuclear magnetic resonance studies of gramicidin A, Biophys. J. 56 (1989) 307–314.
[61] G.V. Miloshevsky, P.C. Jordan, Anion pathway and potential energy profiles along curvilinear bacterial ClC Cl^- pores: electrostatic effects of charged residues, Biophys. J. 86 (2004) 825–835.
[62] J.A. Lundbaek, O.S. Andersen, Lysophospholipids modulate channel function by altering the mechanical properties of lipid bilayers, J. Gen. Physiol. 104 (1994) 645–673.
[63] G. Portella, P. Pohl, B.L. de Groot, Invariance of single-file water mobility in gramicidin-like peptidic pores as function of pore length, Biophys. J. 92 (2007) 3930–3937.
[64] A. Chattopadhyay, D.A. Kelkar, Ion channels and D-amino acids, J. Biosci. 30 (2005) 147–149.
[65] D.A. Doyle, J.M. Cabral, R.A. Pfuetzner, A. Kuo, J.M. Gulbis, S.L. Cohen, B.T. Chait, R. MacKinnon, The structure of the potassium channel: molecular basis of K^+ conduction and selectivity, Science 280 (1998) 69–77.
[66] F. Separovic, J. Gehrmann, T. Milne, B.A. Cornell, S.Y. Lin, R. Smith, Sodium ion binding in the gramicidin A channel. Solid-state NMR studies of the tryptophan groups, Biophys. J. 67 (1994) 1495–1500.
[67] R. Smith, D.E. Thomas, A.R. Atkins, F. Separovic, B.A. Cornell, Solid state 13C NMR studies of the effects of sodium ions on the gramicidin A ion channel, Biochim. Biophys. Acta 1026 (1990) 161–166.
[68] B.A. Wallace, Common structural features in gramicidin and other ion channels, BioEssays 22 (2000) 227–234.
[69] A.S. Arseniev, I.L. Barsukov, V.F. Bystrov, A.L. Lomize, Y.A. Ovchinnikov, ^{1}H NMR study of gramicidin A transmembrane ion channel: head-to-head right-handed, single-stranded helices, FEBS Lett. 186 (1985) 168–174.
[70] M.R.R. De Planque, J.A. Killian, Protein–lipid interactions studied with designed transmembrane peptides: role of hydrophobic matching and interfacial anchoring (review), Mol. Membr. Biol. 20 (2003) 271–284.
[71] L.E. Townsley, W.A. Tucker, S. Sham, J.F. Hinton, Structures of gramicidins A, B, and C incorporated into sodium dodecyl sulfate micelles, Biochemistry 40 (2001) 11676–11686.
[72] W. Hu, T.A. Cross, Tryptophan hydrogen bonding and electric dipole moments: functional roles in the gramicidin channel and implications for membrane proteins, Biochemistry 34 (1995) 14147–14155.
[73] F. Separovic, K. Hayamizu, R. Smith, B.A. Cornell, C 13 chemical shift tensor of L tryptophan and its application to polypeptide structure determination, Chem. Phys. Lett. 181 (1991) 157–162.
[74] F. Separovic, J. Ashida, T. Woolf, R. Smith, T. Terao, Determination of chemical shielding tensor of an indole carbon and application to tryptophan orientation of a membrane peptide, Chem. Phys. Lett. 303 (1999) 493–498.
[75] S. Mukherjee, A. Chattopadhyay, Motionally restricted tryptophan environments at the peptide–lipid interface of gramicidin channels, Biochemistry 33 (1994) 5089–5097.
[76] N.C. Bingham, N.E.C. Smith, T.A. Cross, D.D. Busath, Molecular dynamics simulations of Trp side-chain conformational flexibility in the gramicidin A channel, Biopolymers 71 (2003) 593–600.
[77] S.S. Rawat, D.A. Kelkar, A. Chattopadhyay, Effect of structural transition of the host assembly on dynamics of an ion channel peptide: a fluorescence approach, Biophys. J. 89 (2005) 3049–3058.
[78] F. Separovic, J.A. Killian, T.A. Cross, Modeling the membrane environment for membrane proteins, Biophys. J. 100 (2011) 2073–2074.
[79] S.E. Feller, R.W. Pastor, Constant surface tension simulations of lipid bilayers: the sensitivity of surface areas and compressibilities, J. Chem. Phys. 111 (1999) 1281–1287.